Chapter 8

Crystallization: From the Conformer to the Crystal

J.S. Redinha, A.J. Lopes Jesus, A.A.C.C. Pais and
J. A. S. Almeida

Additional information is available at the end of the chapter

http://dx.doi.org/10.5772/54447

1. Introduction

Crystallization, commonly defined as a process of formation of a crystalline solid from a supersaturated solution, melt or vapor phase, is an old technique widely used in laboratory and in industrial processes to separate and purify substances. In various modern industries, crystalline forms with a certain habit, size and structure, constitute the basic materials for the production of highly sophisticated materials [1, 2]. Integrated circuits as well as piezoelectric and optical materials are just a few examples of devices whose properties are dependent on the crystal structure. Also, in organic chemistry, molecular crystals with determined characteristics are now-a-days of utmost importance for the production of pharmaceuticals, dyestuffs, pigments, foodstuffs, chemicals, cosmetics, etc. For all these reasons, crystal growth has become an important and attractive research field.

Crystallization from solution is one of the preferred methods to obtain a crystal since it can be carried out under different experimental conditions and provides a wide variety of products. In fact, it can occur by lowering the temperature of a supersaturated solution, partial evaporation of the solvent, precipitation by adding an anti-solvent or vapor diffusion of a gas into the solution. Furthermore, solvents with different properties can be used. Such a diversity of experimental conditions has great influence in the output, *i.e.*, in the type of crystalline phase that can be obtained. Therefore, any aprioristic selection of the conditions leading to a desired final product is a fundamental challenge but it is also an almost unfeasible task [3-5]. On respect to the harvest, crystallization is, in a certain extension, a trial-and-error operation.

The various steps of crystallization from solvents are summarized in the following scheme:

Scheme 1. Main crystallization pathways from solution

The competition between the solute-solvent and solute-solute interactions to form the nuclei, and between the specific aggregation forces and packing in order to minimize repulsive interactions, determine the structure of the new crystalline phase. During this process the molecular conformation can change drastically in an unpredicted way. Various computational approaches have been employed to predict the crystalline structure (unit cell, space group and atomic coordinates) formed by a given molecule [6-8], most of them relying on the assumption that the most probable forms are those with lowest lattice energy. Despite the recent success of these methods in the prediction of crystalline structures of small rigid molecules [9], their applicability to high size flexible molecules is not yet satisfactory [10, 11]. The main drawbacks lie in the difficultly of describing accurately the high complexity of inter and intramolecular interactions (e.g. hydrogen bonds and van der Waals interactions) and of selecting, among the energetically feasible polymorphs, that or those that really exist [3]. In truth, crystal prediction is still a very hard task so far.

Nevertheless, computational calculation can be a powerful tool to get information about the different steps of crystallization. The main goal of the present chapter is included in this research field. Quantum-chemical calculations or molecular dynamics simulations, adapted to the molecular complexity can be used for this purpose. In molecular terms, a compound with a certain conformational flexibility exists in a supersaturated aqueous solution as a mixture of conformers with different populations. The knowledge of the conformational equilibrium in this medium is a way of identifying the conformers that are likely to be involved in the early stages of nucleation and to interpret the mechanism of the crystallization process. In this chapter, these topics are addressed by presenting the results obtained for erythritol and *L*-threitol, two isomeric alditols with four carbon atoms, and glutamic acid. These compounds were chosen because of the role played by their conformational features on crystallization. Furthermore, the two polyols exhibit a different crystallization behavior despite being chemically similar. The energies of the different conformers were obtained through theoretical calculations at the DFT level of theory [12, 13] using the popular B3LYP (Becke, 3-parameter, Lee-Yang-Parr) exchange-correlation functional [14-16] combined with the aug-cc-pVDZ [17, 18] or 6-311++G(d,p) [19] basis set. Solvent effects have been accounted by using the well-established conductor-like polarizable continuum model (CPCM) [20-22].

As crystallization proceeds, the self-association of the solute molecules gives rise to molecular aggregates which play an important role in the resulting crystalline structure [23-25]. Data from the application of molecular dynamics simulations in the study of aqueous solutions of erythitol and *L*-threitol near the saturation concentration are reported in an attempt to give an insight into the type of supramolecular species formed in solution, and hence a step forward to elucidate about their crystallization behavior.

http://dx.doi.org/10.5772/54447

As stated before, depending on the experimental conditions and intrinsic molecular features of the molecules, different crystalline phases or polymorphs can be obtained by crystallization. The polymorphs differ from one another in the arrangement (packing) and/or conformation of the molecules in the crystal lattice [26-29]. They are commonly called packing polymorphs in the first case and conformational polymorphs in the second one. Polymorphism has significant implications in a wide range of areas and for this reason it has been matter of extensive investigation. Some typical examples are here reported with the objective of pointing out the diversity of structures that can obtained by crystallization.

2. Nucleation and crystal growth

Fluctuations of the order of a solution, for example density, are accompanied by the formation of solute molecular clusters. The driving force to bring the molecules close together is given by the following chemical potential difference:

$$\mu - \mu^* = kT \ln \frac{C}{C^*} \tag{1}$$

In this equation, μ and μ^* are the chemical potentials of the solute at the actual (C) and saturation (C^*) concentrations, respectively. The Gibbs energy change per molecule (Δg) corresponding to the formation of a spherical cluster of radius r is [30-32]

$$\Delta g = \frac{4/3\pi r^3}{v} \Delta\mu + 4\pi r^2 \sigma \tag{2}$$

where v is the molecular volume and σ the interfacial energy per surface. The first term of the right hand equation gives the work produced by the intermolecular attractive forces (Δg_b) while the second one corresponds to the work required to increase the surface area in 1cm^2 (Δg_s). Owing to the meaning of both terms, equation (2) can be rewritten as

$$\Delta g = \Delta g_b + \Delta g_s \tag{3}$$

With the increase of concentration, the amplitude of the fluctuations also increase and so do the size of the clusters. For smaller size clusters, Δg_s is the dominant contribution and $\Delta g/dr > 0$, *i.e.*, the clusters are unstable. Conversely, for larger size clusters, Δg_b is dominant and $\Delta g/dr < 0$, meaning that the clusters are stable solid particles. The curve representing the variation of Δg with the radius, shown in Figure 1, passes through a maximum at $r = r_c$ ($d\Delta g/dr = 0$), with r_c representing the limiting size for stable clusters. A cluster of this size is the embryo of the solid form nucleus. The following relationships involving r_c can be established:

$$r_c = -\frac{2v\sigma}{\Delta\mu} \quad \text{a}$$
$$r_c = -\frac{2\sigma}{\Delta g_b} \quad \text{b} \tag{4}$$
$$\Delta g_c = \frac{4\pi r_c^2 \sigma}{3} \quad \text{c}$$

where Δg_c corresponds to the value of Δg at r_c. The supersaturation concentration (S) can be related with the clusters size by the Gibbs-Thomson equation:

$$\ln\frac{C}{C^*} = \ln S = \frac{2v\sigma}{kTr_c} \tag{5}$$

Combining (4c) and (5), the following expression is obtained for Δg_c as function of the supersaturation:

$$\Delta g_c = \frac{16\pi\sigma^3 v^2}{3kT\ln S^2} \tag{6}$$

Δg_c represents the energy barrier for the nucleation process and the rate of nucleation (J) will be given by:

$$J = Ae^{\left(\frac{-\Delta g_c}{kT}\right)} \tag{7}$$

This equation shows that the rate of nucleation is strongly dependent on the supersaturation and tends to a finite value for a given supersaturation.

Organic crystals are supramolecules, *i.e*, an ensemble of molecules, bonded by non-covalent forces involving ions, polar or non-polar groups. Such interactions, whatever their strength, do not change the molecular individuality. Hydrogen bonding occupies a special place among the intermolecular interactions occurring in molecular crystals. Its energy ranges from 160 kJ mol^{-1} (strongly covalent) down to 16 kJ mol^{-1} (mostly electrostatic) [33] and it is highly dependent on the orientation of the hydrogen donor group (D–H) relative to the acceptor atom (A). The maximum strength occurs when the D–H···A angle is approximately 180°, though values greater than 110° are acceptable for a hydrogen bond [34].

It is obvious that a crystal packing in which the specific interactions between the functional groups (molecular recognition) are more favorable is, in principle, that leading to the lowest energy. Thus, the lowest energy crystalline structure would correspond to the stronger interac-

http://dx.doi.org/10.5772/54447

tion between a group and its complementar in nature. For example, to a positive charge there would be a negative one, or to a H-bond donor a H-bond acceptor. The molecular packing bringing the molecules close together also gives rise to steric repulsion. Hence, the equilibrium structure is the result between the attraction force and the steric repulsion. This compromise makes the molecule to adopt a conformation corresponding to the lowest Gibbs energy.

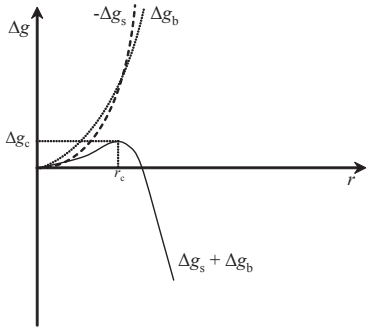

Figure 1. Variation of Δg and its components with the radius of the molecular clusters.

Let us consider the conformational variation from the gas phase to the solid for a simple molecule as paracetamol (acetaminophen). This is a drug of great commercial interest in the pharmaceutical industry owing to its wide use as antipyretic and analgesic agent. This molecule exhibits two relevant conformers differing from one another in the orientation of the OH relatively to the carbonyl group [35]. In one of them the dihedral angle formed by the H-O(1)-C-O(2) atoms is close to 180° (*trans* conformation, Figure 2), while in the other the angle is approximately 0° (*cis* conformation). Geometry optimization of the two conformers followed by vibrational frequencies calculation at the B3LYP/aug-cc-pVDZ level shows that in the gas phase the population (%) of *cis* relative to *trans* is 57:43. Including water effects by applying the CPCM model, both conformers are practically isoenergetic and so their relative population is 50:50. However, in the crystalline phase only the *trans* conformer is presented. This means that the lattice energy yielded by the *trans* conformer is more negative than that of the *cis* conformer. Along this chapter some examples will be given concerning the relationship between the conformers' population in the three states of matter.

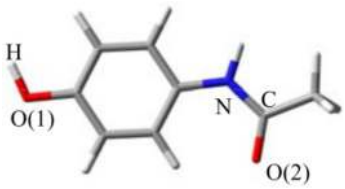

Figure 2. Optimized geometry of the *trans* conformer of paracetamol at the B3LYP/aug-cc-pVDZ level.

3. Polymorphism

According to McCrone [36], polymorphism of a compound corresponds to its ability to crystallize into more than one crystalline structure. From the thermodynamic point of view, only the lowest Gibbs energy form exists. However, higher energy polymorphs can remain as metastable forms for a period of time long enough to be used for practical purposes, providing the height of the energy barrier separating these polymorphs and the most stable one is sufficiently high [28]. Since different solid-state modifications exhibit distinct physicochemical properties, such for example the melting point, solubility, dissolution rate and density, polymorphism has a great impact in the pharmaceutical, food and dyes technologies, among others. For example, in the pharmaceutical industry, the desired polymorph for a given active pharmaceutical ingredient (API) would be the one with highest bioavailability and structural stability during shelf life [37].

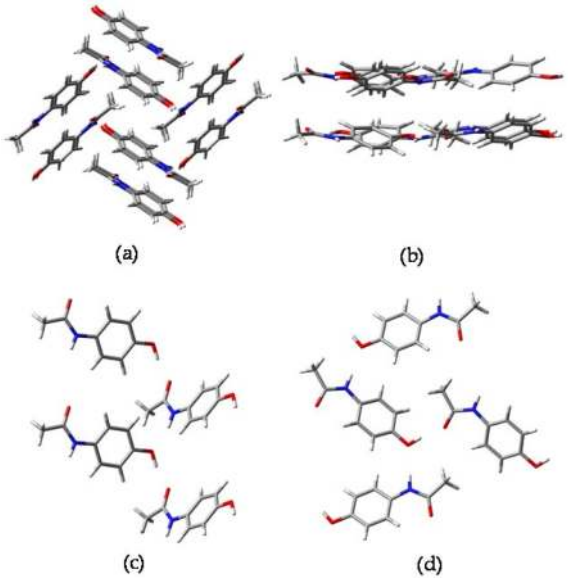

Figure 3. Views of the crystalline structures of forms I (a) and II (b) of paracetamol and detail of the H-bonds formed in both polymorphs [(c) and (d)].

A typical example of a drug exhibiting polymorphism is paracetamol. Three polymorphs, labeled as I, II and III, have been identified for this compound [38-40]. The first (form I) is the thermodynamically stable form while the second (form II) is metastable but exists long enough to be experimentally studied. It is usually prepared from cooled melt [41]. Form III is very unstable [41] and thus it is not possible to investigate its structure and properties. Form I crystallizes in the monoclinic system (space group $P2_1/a$) [42, 43]. As shown in Figure 3, the molecules in the crystalline structure are linked through O–H O=C and N–H O–H hydrogen bonds forming chains which in turn give rise to pleated layers [frames (a) and (a')].

http://dx.doi.org/10.5772/54447

Regarding form II, it crystallizes in the orthorhombic system (space group *Pcab*) [44, 45]. The H-bonding system is identical to that existing in form I but the layers are plane interconnected by van der waals forces [frames (b) and (b')].

The geometric parameters of the H-bonds in forms I and II are summarized in Table 1. In both forms the O–H···O=C hydrogen bond is stronger than the N–H···O–H one. In addition, the hydrogen bonds in the stable polymorph are stronger than in the metastable one.

The two polymorphs were also characterized by infrared spectroscopy [46, 47]. The values of the stretching vibration frequencies for the groups involved in hydrogen bonds are given in Table 2. To work as reference, the frequencies of the "free" groups, obtained from a spectrum of paracetamol in a $CDCl_3$ solution were also included in the Table. From the frequency shift ($\Delta\nu$) of the NH and OH groups one can estimate the enthalpy involved in the two hydrogen bonds by applying the empirical relationship proposed by Iogansen: $\Delta H^2 = 1.92(\Delta\nu - 40)$ [48]. The value of ΔH estimated for the N–H···O–H H-bond was found to be 12 kJ mol^{-1} for both polymorphs, while that estimated for the O–H···O=C one was found to be 28 kJ mol^{-1} for form I and 19 kJ mol^{-1} for form II.

Form	O–H···O=C			N–H···O–H		
	H···O/Å	O···O/Å	O–H···O/º	H···O/Å	N···O/Å	N–H···O/º
I	1.719	2.653	167.5	2.032	2.904	161.6
II	1.838	2.709	170.6	2.069	2.943	163.8

[a] Values taken from ref. [43, 45]

Table 1. Distances and angles of the hydrogen bonds in the paracetamol polymorphs.[a]

	vNH	vOH	vCO
form I	3324	3160	1656
form II	3326	3205	1666 ; 1656
$CDCl_3$ solution	3438	3600	1683

[a] Values taken from ref. [46, 47]

Table 2. Vibrational frequencies (ν/cm^{-1}) corresponding to the NH, OH and CO stretching vibrations of paracetamol in the two crystalline phases and in a $CDCl_3$ solution.[a]

The higher stability of form I is also confirmed by the thermodynamic properties obtained for sublimation, fusion and vaporization of the two polymorphic forms [38]. The value of the packing density, determined by flotation or X-ray (or neutron) diffraction [49] is higher in form II than in form I. In fact, at 298K the density of the former is 1.336 g cm^{-3} while that of the latter is 1.297 g cm^{-3}. That is, the higher stability of form I results from a stronger hydrogen bond interaction rather than from a more favorable packing. In this compound, the differences between specific interactions resulting from the conformational recognition overcome that due to the crystal packing.

The polymorphism of paracetamol assumes great importance from the practical point of view in so far the commercialized polymorph is not the most suitable solid for formulation [45, 50, 51]. Despite it is easily obtained from various solvents, it has the inconvenient to require a binding agent to make tablets for compression. During this process it gives a brittle solid, consequence of its rough molecular layers. Conversely, form II is constituted by thin plates that glide on pressing. Its plasticity allows the formulation into tablets by direct compression without the need of incorporating any binder agent [45]. The main difficulty to obtain this form comes up against the existence of an adequate method for their preparation at an industrial scale [41].

Aspirin (acetylsalicylic acid) is a drug commonly used as analgesic, antipyretic and anti-inflammatory. It is also known to act as anticoagulant by reducing the blood platelet aggregation [52]. About 35,000 tons of aspirin are taken a day throughout the world.

Using X-ray diffraction, the structure of aspirin has been characterized for the first time in 1964 as a monoclinical crystal, space group P21/c [53]. In 2004, the existence of a second polymorph (form II) was predicted computationally [54] and observed experimentally one year later [55]. However, in view of the slight differences between both structural modifications, it was speculated that this new form might result from uncertainties of the methods used in the structural characterization [56, 57]. Just recently it has been settled the existence of a second polymorph for this compound [58]. In both forms, the carboxyl groups of two neighbor molecules are connected by O–H···O=C H-bonds giving rise to centrosymmetric dimers as illustrated in Figure 4. These dimers are arranged into stacked layers, which are identical in the two polymorphs. The acetyl groups of molecules belonging to different layers are in turns interconnected through C–H···O interactions. In Form I, these interactions have centrosymmetric geometry, *i.e.*, the CH_3 and CO groups of one molecule are bonded to the complementary groups of a neighbor molecule. The structure is a sequence of AAAA layers. Unlike, the structure of form II is a sequence of ABAB layers [59]. The difference between the B and A layers lies in a relative translation of the lattice repetition. This means that in the latter form the CH_3 and CO groups of one molecule are connected to the complementary groups of two neighbor molecules, yielding catemers.

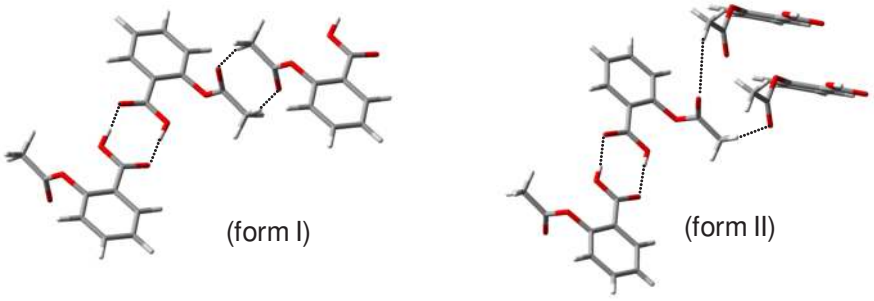

Figure 4. H-bonds in the crystalline structures of forms I and II of aspirin.

http://dx.doi.org/10.5772/54447

An interesting feature of aspirin single crystals is that they exhibit simultaneously domains of forms I and II of variable relative size. Deran *et al*. [58] explain this type of behavior as an accidental degeneracy. According to these authors the two polymorphs are isoenergetic and during crystallization an intergrowth of both forms occurs. The more favorable internal conformation in form I is compensated by an enhanced cooperativity of the catameric H-bonding network in form II. These results raise the question of whether or not these two forms of aspirin can be called polymorphs. According to the definition given by McCrone [36], they do not fit into the concept.

Besides polymorphism, further crystalline structure complexity arises with the existence of disorder in crystals, situation quite common in many organic crystals [60-64]. This occurs when portions of the structure under analysis occupy two or more positions. For example, molecular fragments of organic molecules not involved in intermolecular interactions can be free enough to acquire different conformations. Such solids are designated by the conflicting denomination of disordered crystals. An example of a compound exhibiting crystal disorder is betaxolol hydrochloride, 1-{4-[2-(cyclopropylmethoxy)ethyl]phenoxy}-3-isopropyl-amino-2-propanol hydrochloride (Figure 5). It is a cardio selective β adrenergic drug that crystallizes into the triclinic system with P_1 symmetry [65].

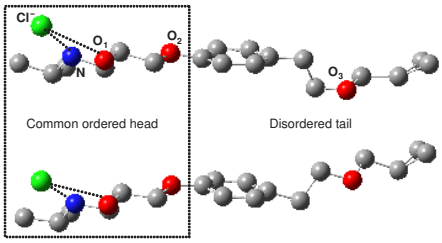

Figure 5. Conformations of betaxolol hydrochloride in the crystalline structure. Hydrogen bonds between the amino and hydroxyl groups with the chloride ion of the same molecule are represented by dotted lines. For better visualization the hydrogen atoms are not shown.

The intermolecular arrangement in the crystalline structure is as follows: the NH_2^+ and the OH groups of the isopropylaminoethanol moiety form H-bonds with the chloride ion of the same molecule as shown in Figure 5. In addition, one of the hydrogens of the NH_2^+ group is also H-bonded to oxygen atom of the OH group of a second molecule while the other hydrogen of the same group is linked to the chloride ion of a third molecule [63, 64]. That is, the betaxolol molecules are connected each other just through the isopropylaminoethanol fragment, leaving a long molecular chain free to move. The X-ray diffraction data shows the existence of an ordered head from the isopropyl group up to O_2 and a disordered tail from this atom to the end. By refinement, the crystalline structure can be satisfactory interpreted as being constituted by two conformations which are displayed in Figure 5. Since we have a no well defined unit cell, the structure of betaxolol hydrochloride can not be included in the polymorphism or isomorphism definitions.

4. Erythritol and threitol: identical chemical structure, different crystalline assembling

Erythritol and *L*-threitol (see Figure 8) are two diastereomers of 1,2,3,4-butanetetrol. The first is a *meso* compound while the second is optically active, existing as *D*- or *L*-threitol. An important difference between both alditols lies in their crystallization ability. Whilst erythritol is easily crystallized from aqueous solution or melt, *L*-threitol is much more difficult to crystallize [66, 67]. As illustrated in the DSC curves shown in Figure 6, molten erythritol transforms readily into a crystalline phase providing it is cooled at scanning rates lower than or equal to 10°C/min. On the contrary, no crystallization peak is observed for *L*-threitol, even when the melt is cooled very slowly, say 2°C/min. Since the two compounds are chemically similar, their different crystallization tendency is likely to have a conformational origin [68].

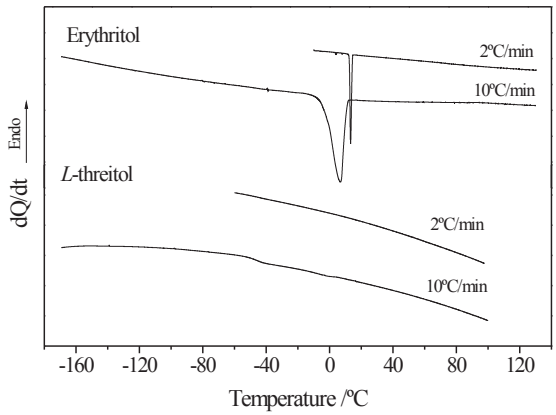

Figure 6. DSC cooling curves of molten erythritol (m.p = 118°C) and *L*-threitol (m.p= 89°C) obtained at different cooling rates

Conformationally, both diastereomers are highly flexible. In fact, the existence of seven independent dihedral angles, each of them assuming three standard orientations: gauche^{+} (60°), gauche^{-} (-60°) and trans (180°), originate a total of 2187 possible conformers. Such a large number of structures make their systematic exploration by means of *ab initio* calculations unfeasible. Therefore, a previous conformational search method using random generation and subsequent molecular mechanics energy minimization has been employed to sampling the most relevant conformations. All generated structures falling within an energy window of 20 kJ mol^{-1} above the global minimum have been then optimized at DFT level using the B3LYP functional and the 6-311++G(d,p) basis set. In order to simulate solvent effects, their energy was also evaluated by single-point calculations in aqueous solution using the CPCM continuum model. Details of the computational calculations are given elsewhere [69, 70].

http://dx.doi.org/10.5772/54447

The Boltzmann populations of the erythritol and *L*-threitol conformers in gas phase and aqueous solution are displayed in Figure 7. The geometries of the relevant conformers in both media, as well as the conformations exiting in the crystalline structures, are depicted in Figure 8. For the sake of simplicity the conformers were grouped according to their backbone family, being labeled with three italic letters: *g* (gauche$^+$), *g'* (gauche$^-$) and *t* (trans), to specify the orientation of the O(1)-C(1)-C(2)-O(2), C(1)-C(2)-C(3)-C(4) and O(3)-C(3)-C(4)-O(4) dihedrals, respectively.

As shown in Figure 7, isolated erythritol exists preferentially in the *tgg* and *ggg* bent conformations (both make up 38% of the conformational mixture at 298.15K). Their stability results from the formation of intramolecular hydrogen bonds which are particularly strong in the *tgg* conformers due to the participation of the terminal OH groups. In the presence of the solvent, the population of these conformers decreases significantly (11%). Conversely, two higher energy conformers in gas phase (*g'tg* and *gtg*), both with a distended carbon backbone, emerge as the most stable forms in solution (49%). This population change can be explained by the stronger hydration of conformers with the OH groups less internally H-bonded and therefore more available to interact with water. In the crystal, the neutron diffraction data available for this compound indicates that the molecule exhibits two conformations, labeled as A and B, differing each other by the positions of the H[O(2)] and H[O(3)] hydrogen atoms. At 22.6 K the occupancy of conformations A and B are 85% and 15%, respectively [71]. In terms of backbone, both have a *g'tg* conformation which is the same as that exhibited by the preferred conformers of erythritol in aqueous solution. As shown in Figure 8, the geometry of the most stable conformer in solution matches that of the crystal conformation having the highest occupancy percentage.

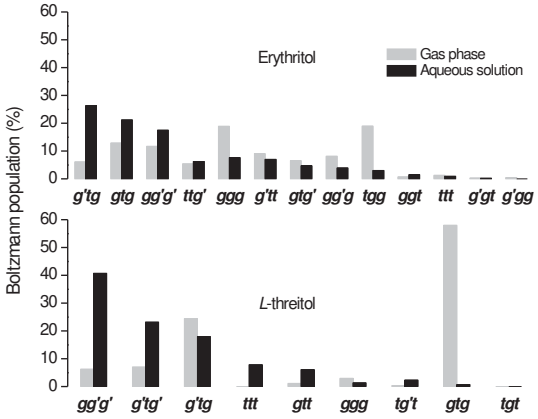

Figure 7. Conformational distribution of erythritol and *L*-threitol in gas phase and aqueous solution. Boltzmann populations were estimated from the Gibbs energies of the conformers [B3LYP/6-311++G(d,p)] in both media.

Regarding *L*-threitol, its gas phase conformational mixture is largely dominated by the *gtg* conformers which are characterized by a cyclic, symmetric and cooperative hydrogen bonding network. Since this OH groups' arrangement is very unfavorable to interact with water, they practically disappear in solution and are replaced by the *gg'g'*, *g'tg'* or *g'tg* conformations which are not so highly intramolecularly bonded. Unlike erythritol, none of these conformations has been identified in the crystalline *L*-threitol [72]. Here, the molecules adopt a distended conformation (*ttt*) which has a relatively low weight in solution (8%) and does not exist in the vacuum.

The results just presented provide an important basis to understand the different crystallization ability of erythritol and *L*-threitol. In the *meso* form, this process is facilitated due to the resemblance between the backbone conformation of the molecules existing in the crystal lattice and that characteristic of the predominant forms in solution. The fact that such resemblance is not found to exist in *L*-threitol may contribute to its lower crystallization tendency. This behavior is in agreement with the results obtained for other alditols [68, 73]

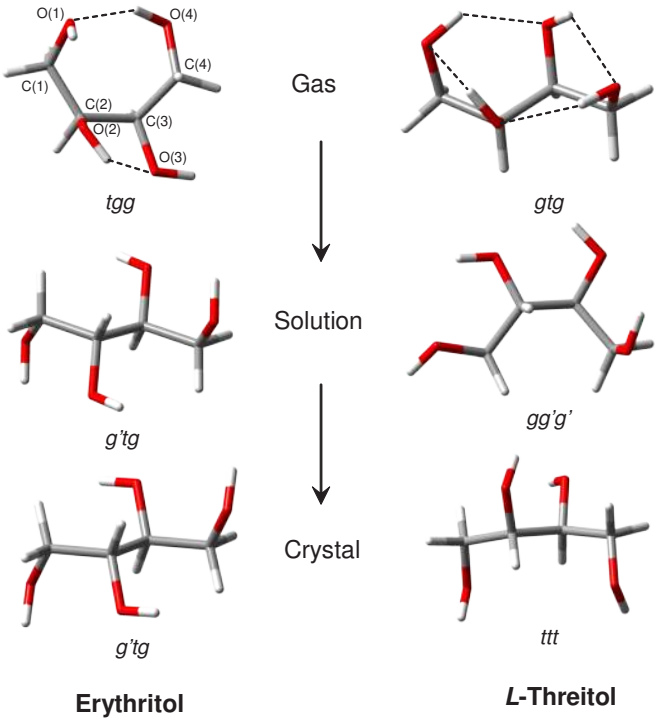

Figure 8. Most stable conformers of erythritol and *L*-threitol in gas phase and aqueous solution, as well as the respective crystal conformations. The crystal conformation of erythritol corresponds to that having highest occupancy in the crystal lattice (Conformation A).

http://dx.doi.org/10.5772/54447

5. Conformational variation during the molecular incorporation into the crystal: Glutamic acid

Glutamic acid, 2-aminopentanedioic acid ($C_5H_9NO_4$), is another example illustrating the role played by conformation on crystallization. Two conformational polymorphs have been identified for this compound, labeled as α and β, with the latter being the thermodynamically stable form over all temperature range [74-77]. The crystals have different morphologies: the metastable form exhibits a prismatic shape while the stable one has a needle-like shape. Both belong to the ortorrombic space group with four molecules in the unit cell (Z=4) [78, 79]. In the crystal lattice the molecules are in the zwitterionic state and all functional groups participate in a complex intermolecular hydrogen bonding network [63].

The conformations adopted by the *L*-glutamic acid molecules in the two polymorphs are displayed in Figure 9. Their main difference lies in the orientation of the two C-C-C-C dihedral angles. In the crystal lattice the C(1)-C(2)-C(3)-C(4) and C(2)-C(3)-C(4)-C(5) dihedrals assume, respectively, values of 59.2°, 68.3° in α and -171.1°, -73.1° in β. Using the same dihedral labeling scheme previously adopted for the polyols, the conformation of glutamic acid in the α and β-crystals is *gg* and *tg'*, respectively. Depending on the experimental conditions, namely the temperature, both polymorphs can be crystallized from aqueous solution. Cooling a supersaturated solution to temperatures below 25°C originates almost pure α-crystals, whereas as the temperature raises the proportion of form β in the precipitated crystals increases. For example at 45°C, the fraction of β-crystals is 45% [74, 75].

The conformational behavior of zwitterionic glutamic acid is aqueous solution is a useful starting point to understand the crystallization of this compound in molecular terms. This has been done theoretically by performing full geometry optimizations using the CPCM continuum solvation model and the B3LYP/aug-cc-pVDZ model chemistry, both implemented in the Gaussian 03 program. The cavity was built with the Bondii radii which have been found to yield accurate results for the hydration of similar molecules in the zwitterionic state, such for example glycine [80]. Nine starting geometries were built by assuming the three standard orientations (*g*, *g'* and *t*) for each one of the C-C-C-C dihedrals. The remaining dihedrals were kept in their preferred orientations. The optimized structures were further submitted to a vibrational frequency calculation at the same level to ensure that they correspond to minima on the aqueous potential energy surface and also to calculate the thermal corrections at 298.15K.

The Gibbs energies of the conformers in aqueous solution at 298.15 K (G_{sol}) can be expressed as: $G_{sol} = E_{int} + \Delta G_{thermal} + \Delta G_{hyd}$, with E_{int} representing the intrinsic (abbreviated as "int") electronic energy of the conformer at 0 K, *i.e.*, excluding solvent effects, $\Delta G_{thermal}$ the thermal correction to the Gibbs energy from 0 to 298K and ΔG_{hyd} the Gibbs energy of hydration at 298.15K. The values of E_{int}, G_{sol}, ΔG_{hyd}, as well as the equilibrium populations at 298.15 K, are given in Table 3. In this table are also included the values of the C(1)-C(2)-C(3)-C(3) and C(2)-C(3)-C(4)-C(5) dihedrals, abbreviated as D(1) and D(2), respectively. The relative stability of the conformers in solution is governed by a balance between two effects: interaction with the solvent (quantified by ΔG_{hyd}) and intramolecular interaction (quantified by E_{int}). In general, conformers with a favora-

ble intramolecular interaction are weakly hydrated and *vice-versa*. The most abundant conformer in solution, *tg* (Pop. = 67%), is the one having a less negative ΔG_{hyd}; however, the intrinsic energy decrease arising from the formation of an internal N^+–H···O hydrogen bond (see Figure 9), turns it into the lowest energy conformer. Unlike, the second most stable conformer (*tt*) has a fully distended backbone that hampers the formation of the just referred intramolecular hydrogen bond and so it has a relatively high intrinsic energy. Its stabilization results essentially from a favorable interaction with the solvent. Both conformers represent *ca*. 81% of the conformational composition in aqueous solution at 298.15K.

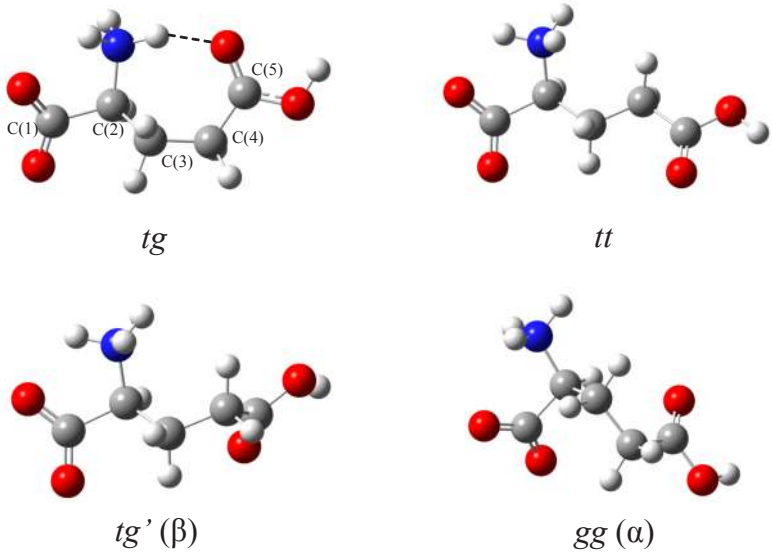

Figure 9. CPCM/B3LYP/aug-cc-pVDZ optimized geometries of relevant conformers of the zwitterionic glutamic acid in aqueous solution. Dashed line represents an intramolecular hydrogen bond. Atom numbering scheme is shown for the most stable conformer.

Regarding the two crystal conformations, *tg'* (β) and *gg* (α), they are stable forms in aqueous solution with the values of the C-C-C-C dihedral angles in solution not differing significantly from those in the crystal. However, somehow surprisingly, their estimated equilibrium populations in solution are too low: 2.3 and 0.2% for conformers β and α, respectively. Glutamic acid thus constitutes an interesting example of a molecule where the conformers experimentally observed in the crystalline structure are much diluted in aqueous solution. Two immediate conclusions can be drawn from this result: (1) the conformational composition in aqueous solution does not determine the conformations exhibited by this compound in the final crystalline state; (2) crystallization is accompanied by a conformational change. The second conclusion implies that conformers *tg* and *tt*, namely the first, are interconverted into the *gg* and *tg'*. These interconversions can be characterized by the energy barriers ($\Delta G^{\ddagger}$) separating these conformers. For

http://dx.doi.org/10.5772/54447

this purpose, we have used the synchronous transit-guided quasi-Newton method (STQN) [81] in its QST2 variety at the CPCM/B3LYP/aug-cc-pVDZ level. The activation energies corresponding to the interconversion of the most stable conformer into conformers α and β were calculated to be $\Delta G^{\ddagger}$ = 18 and 29 kJ mol^{-1}, respectively. This barrier height difference may help to explain the preferential crystallization of form α at temperatures below 25°C and the increase of the percentage of form β in the crystals obtained at higher temperatures. Apparently, the dependence of the crystallization behavior of glutamic acid on temperature is not due to a change on the relative abundance of the crystallizing conformers in solution with temperature [75], but rather to the value of the energy barriers for the interconversion of the most stable conformer in solution into the α and β conformers.

Conf.	Dihedral angles/º		E_{int}/ kJ mol^{-1}	$-\Delta G_{hyd}$/ kJ mol^{-1}	G_{sol}/ kJ mol^{-1}	Pop. (%)
	D(1)	D(2)				
tg	178.5	75.3	13.1	184.8	0.0	67.1
tt	168.9	-177.2	56.9	223.7	3.9	13.6
g′g′	-52.5	-79.9	0.0	168.2	4.8	9.8
gt	63.1	178.8	36.4	196.1	7.4	3.5
g´t	-56.5	178.7	52.1	213.7	7.7	3.0
tg′(β)	172.5	-69.8	59.6	221.9	8.4	2.3
gg′	62.4	-85.1	49.8	208.1	12.5	0.4
gg(α)	66.1	61.1	54.7	210.5	14.0	0.2
g´g	-61.7	81.4	71.1	225.3	18.3	0.0

Table 3. Dihedral angles, intrinsic electronic energies at 0K (E_{int}), Gibbs energies in aqueous solution (G_{sol}), Gibbs energies of hydration (ΔG_{hyd}) and Boltzmann populations (Pop.) at 298.15K of the zwitterionic glutamic acid conformers, calculated at the CPCM/B3LYP/aug-cc-pVDZ level.

6. Molecular dynamics study of pre-nucleation clusters

The molecular aggregates individualized in the early stages of nucleation (pre-nucleation) are windows to follow the crystallization process. Data on the self-assembly of erythritol and *L*-threitol in supersaturated aqueous solutions are reported through molecular dynamics (MD) simulations. MD is one of the most comprehensive computer simulation tools, with enormous application in the study of large systems and molecular phenomena requiring longer observation times. Relevant molecular phenomena are often adequately described by classical mechanics, providing reliable force-fields are available for a variety of systems. The results of the MD simulations presented in this chapter were carried out in the NpT ensemble and under periodic boundary conditions, resorting to the GROMACS package, version 4.5.4 [82] and GROMOS 96 43a1 force field [83]. Long-range electrostatics was computed using the particle mesh Ewald (PME) method, while for Lennard-Jones energies a cut-off of 1.4

nm was applied. Temperature (298K) and pressure (1bar) were coupled to Berendsen external baths, with coupling constants of 0.1 and 0.5 ps, respectively. Each system was firstly subjected to an energy minimization step, and then left to evolve up to 80ns, using in both parts a standard time step of 2 fs. The last 40 ns of production runs were subsequently subjected to standard analysis, such as radial distribution functions [RDF, g(*r*)].

Useful data about the type of aggregates formed in solution can be given by the RDFs for the different pairs of solute OH groups (OH–OH) which are depicted in Figure 10. They were obtained from the simulation of an aqueous solution containing 11 solute molecules and 4000 solvent molecules, corresponding to a concentration of 75g /100 cm^3, which is near to the saturation concentration [84].

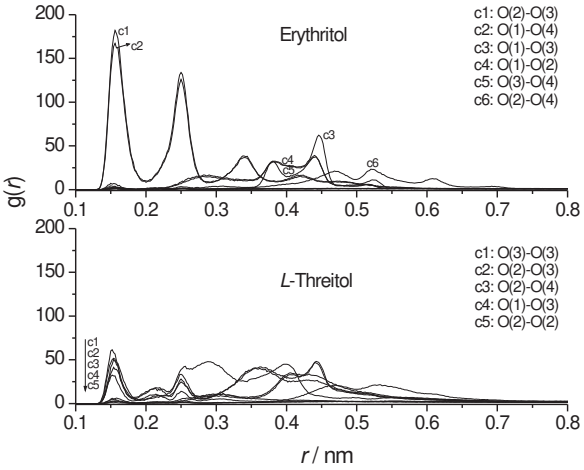

Figure 10. OH–OH RDFs for erythritol and *L*-threitol in aqueous solution. For better visualization the most relevant curves are numbered as c1, c2, etc.

In erythritol, the most prominent RDFs are found for the O(2)H–O(3)H and O(1)H–O(4)H pairs. Both RDFs, labeled in Figure 10 as c1 and c2, respectively, exhibit sharp and intense peaks at *r* (nearest distance between groups) = 0.16 and 0.25 nm. This indicates that the self-assembly of erythritol in solution yields well organized clusters formed by hydrogen bonds involving preferentially the O(1)H and O(4)H groups or the O(2)H and O(3)H groups. Analysis of the MD trajectory shows that these clusters are mostly dimers with some of them involving simultaneously the two just referred H-bonds (cyclic dimers). Interestingly, the cyclic dimer formed by these two H-bonds is the one existing in the crystalline structure. Some illustrative snapshots of these dimers are displayed in Figure 11. From the other OH–OH RDFs shown in Figure 10 one can conclude that the formation of intermolecular hydrogen bonds involving the remaining groups is very unlikely to occur. In fact, the integration

http://dx.doi.org/10.5772/54447

of all RDFs up to 0.28 nm (cut-off distance for the formation of an H-bond [85]) reveals that their probability of formation is lower than 15%.

Regarding *L*-threitol, the RDF profiles are substantially different from those obtained for erythritol. In fact, the most relevant RDFs, labeled in Figure 10 as c1 to c5 and corresponding to the O(3)H–O(3)H, O(2)H–O(3)H, O(2)H–O(4)H, O(1)H–O(3)H and O(2)H–O(2)H interactions, show relatively well defined first peaks centered at 0.15 nm. The first peaks heights are much lower than in erythritol which means that the organized part of the *L*-threitol clusters is much smaller as compared to that in erythitol. The remaining part of the clusters has a disordered structure as evidenced by the broad peaks located at larger distances. This result is an argument in favor of the lower crystallization tendency of this compound, in addition to the conformational one discussed in section 4. The snapshots of *L*-threitol clusters during the simulation show the existence of various types of disordered oligomers (Figure 12).

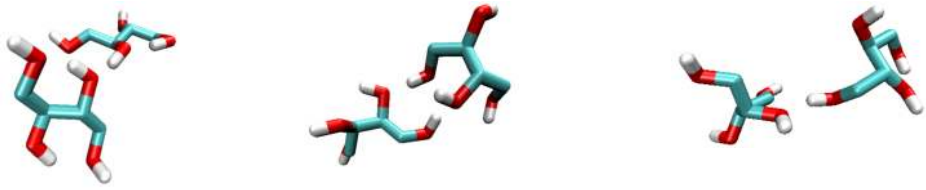

Figure 11. Snapshots of the erythritol clusters formed in aqueous solution.

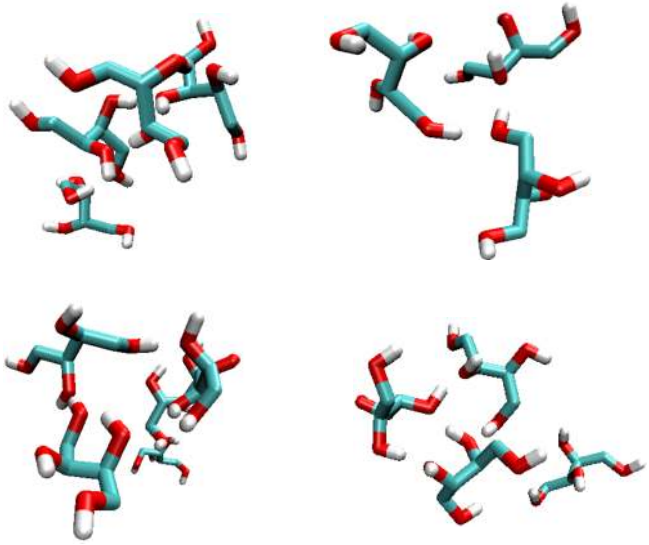

Figure 12. Snapshots of the *L*-threitol clusters formed in aqueous solution.

7. Conclusion

Structural aspects of crystallization from solvents were pointed out throughout this chapter. Particular attention was paid to the conformational variation of flexible molecules during this process. Three compounds were taken as examples: erythritol, *L*-threitol and glutamic acid. The different crystallization behavior shown by the two alditols was understood in terms of the resemblance between the solution and crystal conformers. Regarding glutamic acid, it is a quite peculiar example since the conformers existing in the two identified conformational polymorphs have a negligible weight in aqueous solution. Their selective crystallization has been interpreted on the grounds of the energy barriers separating the dominant conformer in solution and those found in both crystalline forms.

The investigation of the structure of the molecular aggregates formed in solution by molecular dynamics, here exemplified for erythritol and *L*-threitol, has proven to be a valuable contribution to better understand crystallization.

Polymorphism, an important property of the solid state structure with various practical implications, was called in the present chapter as a tangly pathway in the crystallization process. Additional crystalline structure complexity may result from crystal disorder, hardly to be included in the polymorphism concept.

Author details

J.S. Redinha[1], A.J. Lopes Jesus[1,2], A.A.C.C. Pais[1] and J. A. S. Almeida[1]

1 University of Coimbra / Department of Chemistry, Portugal

2 University of Coimbra / Faculty of Pharmacy, Portugal

References

[1] Brian Henderson and Ralph HB. Crystal-Field Engineering of Solid-State Laser Materials. New York: Cambridge University Press; 2000.

[2] Brooks JS. Organic crystals: properties, devices, functionalization and bridges to biomolecules. Chemical Society Reviews. 2010;39(7):2667-94.

[3] Day GM, Motherwell WDS, Ammon HL, Boerrigter SXM, Della Valle RG, Venuti E, et al. A third blind test of crystal structure prediction. Acta Crystallographica Section B. 2005;61(5):511-27.

[4] Motherwell WDS, Ammon HL, Dunitz JD, Dzyabchenko A, Erk P, Gavezzotti A, et al. Crystal structure prediction of small organic molecules: a second blind test. Acta Crystallographica Section B. 2002;58(4):647-61.

[5] Lommerse JPM, Motherwell WDS, Ammon HL, Dunitz JD, Gavezzotti A, Hofmann DWM, et al. A test of crystal structure prediction of small organic molecules. Acta Crystallographica Section B. 2000;56(4):697-714.

[6] Oganov AR, editor. Modern Methods of Crystal Structure Predictions. Weinheim: Wiley-VCH; 2011.

[7] Woodley SM, Catlow R. Crystal structure prediction from first principles. Nature Materials. 2008;7(12):937-46.

[8] Oganov AR, Glass CW. Crystal structure prediction using ab initio evolutionary techniques: Principles and applications. Journal of Chemical Physics. 2006;124(24): 244704-15.

[9] Day GM, Cooper TG, Cruz-Cabeza AJ, Hejczyk KE, Ammon HL, Boerrigter SXM, et al. Significant progress in predicting the crystal structures of small organic molecules - a report on the fourth blind test. Acta Crystallographica Section B. 2009;65(2): 107-25.

[10] Kim S, Orendt AM, Ferraro MB, Facelli JC. Crystal structure prediction of flexible molecules using parallel genetic algorithms with a standard force field. Journal of Computational Chemistry. 2009;30(13):1973-85.

[11] Day GM, S. Motherwell WD, Jones W. A strategy for predicting the crystal structures of flexible molecules: the polymorphism of phenobarbital. Physical Chemistry Chemical Physics. 2007;9(14):1693-704.

[12] Hohenberg P, Kohn W. Inhomogeneous Electron Gas. Physical Review. 1964;136(3B):B864-B71.

[13] Kohn W, Sham LJ. Self-Consistent Equations Including Exchange and Correlation Effects. Physical Review. 1965;140(4A):A1133-A8.

[14] Becke AD. Density-Functional Exchange-Energy Approximation with Correct Asymptotic-Behavior. Physical Review A. 1988 Sep 15;38(6):3098-100.

[15] Becke AD. Density-Functional Thermochemistry.3. The Role of Exact Exchange. Journal of Chemical Physics. 1993 Apr 1;98(7):5648-52.

[16] Lee CT, Yang WT, Parr RG. Development of the Colle-Salvetti Correlation-Energy Formula into a Functional of the Electron-Density. Physical Review B. 1988 Jan 15;37(2):785-9.

[17] Dunning J, Thom H. Gaussian basis sets for use in correlated molecular calculations. I. The atoms boron through neon and hydrogen. Journal of Chemical Physics. 1989 1989/01/15/;90(2):1007-23.

[18] Woon DE, Dunning J, Thom H. Gaussian basis sets for use in correlated molecular calculations. III. The atoms aluminum through argon. Journal of Chemical Physics. 1993 1993/01/15/;98(2):1358-71.

[19] Krishnan R, Binkley JS, Seeger R, Pople JA. Self-consistent molecular orbital methods. XX. A basis set for correlated wave functions. Journal of Chemical Physics. 1980;72(1):650-4.

[20] Cossi M, Rega N, Scalmani G, Barone V. Energies, structures, and electronic properties of molecules in solution with the C-PCM solvation model. Journal of Computational Chemistry. 2003 Apr 30;24(6):669-81.

[21] Cossi M, Barone V, Cammi R, Tomasi J. Ab initio study of solvated molecules: A new implementation of the polarizable continuum model. Chemical Physics Letters. 1996 Jun 14;255(4-6):327-35.

[22] Klamt A, Schuurmann G. Cosmo - a New Approach to Dielectric Screening in Solvents with Explicit Expressions for the Screening Energy and Its Gradient. Journal of the Chemical Society- Perkin Transactions 2. 1993(5):799-805.

[23] Weissbuch I, Kuzmenko I, Vaida M, Zait S, Leiserowitz L, Lahav M. Twinned Crystals of Enantiomorphous Morphology of Racemic Alanine Induced by Optically Resolved.alpha.-Amino Acids; A Stereochemical Probe for the Early Stages of Crystal Nucleation. Chemistry of Materials. 1994 2012/09/14;6(8):1258-68.

[24] Etter MC. Hydrogen bonds as design elements in organic chemistry. Journal of Physical Chemistry. 1991 2012/09/14;95(12):4601-10.

[25] Weissbuch I, Lahav M, Leiserowitz L. Toward Stereochemical Control, Monitoring, and Understanding of Crystal Nucleation. Crystal Growth & Design. 2003 2012/09/14;3(2):125-50.

[26] Bernstein J. Polymorphism in Molecular Crystals. Oxford: Oxford University Press; 2002.

[27] Hilfiker R, editor. Polymorphism in the Pharmaceutical Industry. Weinheim: Willey-VCH; 2006.

[28] Brittain HG, editor. Polymorphism in Pharmaceutical Solids. 2 ed. New York: Informa Healthcare USA, Inc; 2009.

[29] Nangia A. Conformational Polymorphism in Organic Crystals. Accounts of Chemical Research. 2008;41(5):595-604.

[30] J.W.Mullin. Crystallization. 4 ed. Oxford: Butterworth-Heinemann; 2001.

[31] Schmelzer JWP, editor. Nucleation Theory and Applications: WILEY-VCH; 2005.

[32] Laaksonen A, Talanquer V, Oxtoby DW. Nucleation: Measurements, Theory, and Atmospheric Applications. Annual Review of Physical Chemistry. 1995;46(1):489-524.

[33] Steiner T. The hydrogen bond in the solid state. Angewandte Chemie, International Edition in English. 2002;41(1):48-76.

[34] Elangannan Arunan, Gautam R. Desiraju, Roger A. Klein, Joanna Sadlej, Steve Scheiner, Ibon Alkorta, et al. Definition of the hydrogen bond (IUPAC Recommendations 2011). Pure and applied chemistry. 2011;83(8):1637-41.

[35] Lee SJ, Min A, Kim Y, Ahn A, Chang J, Lee SH, et al. Conformationally resolved structures of jet-cooled acetaminophen by UV-UV hole-burning spectroscopy. Physical Chemistry Chemical Physics. 2011;13(37):16537-41.

[36] McCrone WC. In: Fox D, Labes MM, Weissberger A, editors. Physics and Chemistry of the Organic Solid State. London: Interscience Publishers; 1965. p. 725-67.

[37] Singhal D, Curatolo W. Drug polymorphism and dosage form design: a practical perspective. Advanced Drug Delivery Reviews. 2004;56(3):335-47.

[38] Perlovich G, Volkova T, Bauer-Brandl A. Polymorphism of paracetamol. Journal of Thermal Analysis and Calorimetry. 2007;89(3):767-74.

[39] Kolesov BA, Mikhailenko MA, Boldyreva EV. Dynamics of the intermolecular hydrogen bonds in the polymorphs of paracetamol in relation to crystal packing and conformational transitions: a variable-temperature polarized Raman spectroscopy study. Physical Chemistry Chemical Physics. 2011;13(31):14243-53.

[40] Boldyreva E, Drebushchak V, Paukov I, Kovalevskaya Y, Drebushchak T. DSC and adiabatic calorimetry study of the polymorphs of paracetamol. Journal of Thermal Analysis and Calorimetry. 2004;77(2):607-23.

[41] Di Martino P, Conflant P, Drache M, Huvenne JP, Guyot-Hermann AM. Preparation and physical characterization of forms II and III of paracetamol. Journal of Thermal Analysis and Calorimetry. 1997;48(3):447-58.

[42] Haisa M, Kashino S, Kawai R, Maeda H. The Monoclinic Form of p-Hydroxyacetanilide. Acta Crystallographica Section B-Structural Science. 1976;32(4):1283-5.

[43] Bouhmaida N, Bonhomme F, Guillot B, Jelsch C, Ghermani NE. Charge density and electrostatic potential analyses in paracetamol. Acta Crystallographica Section B. 2009;65(3):363-74.

[44] Haisa M, Kashino S, Maeda H. The orthorhombic form of p-hydroxyacetanilide. Acta Crystallographica Section B. 1974;30(10):2510-2.

[45] Nichols G, Frampton CS. Physicochemical characterization of the orthorhombic polymorph of paracetamol crystallized from solution. Journal of Pharmaceutical Sciences. 1998;87(6):684-93.

[46] Burgina EB, Baltakhinov VP, Boldyreva EV, Shakhtschneider TP. IR Spectra of Paracetamol and Phenacetin. 1. Theoretical and Experimental Studies. Journal of Structural Chemistry. 2004;45(1):64-73.

[47] Ivanova BB. Monoclinic and orthorhombic polymorphs of paracetamol - solid state linear dichroic infrared spectral analysis. Journal of Molecular Structure. 2005;738(1-3):233-8.

[48] Iogansen AV. Direct proportionality of the hydrogen bonding energy and the intensification of the stretching v(XH) vibration in infrared spectra. Spectrochimica Acta, Part A: Molecular and Biomolecular Spectroscopy. 1999;55(7-8):1585-612.

[49] Wendy C. Duncan-Hewitt, Grant DJW. True density and thermal expansivity of pharmaceutical solids: comparison of methods and assessment of crystallinity. International Journal of Pharmaceutics. 1986;28(1):75-84.

[50] Joiris E, Martino PD, Berneron C, Guyot-Hermann A-M, Guyot J-C. Compression Behavior of Orthorhombic Paracetamol. Pharmaceutical Research. 1998;15(7):1122-30.

[51] Di Martino P, Guyot-Hermann AM, Conflant P, Drache M, Guyot JC. A new pure paracetamol for direct compression: The orthorhombic form. International Journal of Pharmaceutics. 1996;128:1-8.

[52] Roth GJ, Calverley DC. Aspirin, Platelets, and Thrombosis: Theory and Practice. Blood. 1994;83(4):885-98.

[53] Wheatley PJ. The crystal and molecular structure of aspirin. Journal of the Chemical Society (Resumed). 1964:6036-48.

[54] Ouvrard C, Price SL. Toward Crystal Structure Prediction for Conformationally Flexible Molecules: The Headaches Illustrated by Aspirin. Crystal Growth & Design. 2004;4(6):1119-27.

[55] Vishweshwar P, McMahon JA, Oliveira M, Peterson ML, Zaworotko MJ. The Predictably Elusive Form II of Aspirin. Journal of the American Chemical Society. 2005 2012/09/10;127(48):16802-3.

[56] Bond AD, Boese R, Desiraju GR. On the Polymorphism of Aspirin. Angewandte Chemie International Edition. 2007;46(4):615-7.

[57] Chang C-J, Díaz LE, Morin F, Grant DM. Solid-state 13C NMR study of drugs: Aspirin. Magnetic Resonance in Chemistry. 1986;24(9):768-71.

[58] Wen S, Beran GJO. Accidental Degeneracy in Crystalline Aspirin: New Insights from High-Level ab Initio Calculations. Crystal Growth & Design. 2012 2012/09/10;12(5):2169-72.

[59] Bond AD, Boese R, Desiraju GR. What Is A Polymorph? Aspirin As A Case Study. American Pharmaceutical Review. 2007:1-4.

[60] Glusker JP, Lewis M, Rossi M. Crystal Structure Analysis for Chemists and Biologists (Methods in Stereochemical Analysis). New York: Wiley-VCH; 1994.

[61] Wilson CC. A basic introduction to thermal motions of atoms in crystal structures, the underlying potentials and the physical information available from their analysis. Crystallography Reviews. 2009 2012/09/11;15(1):3-56.

[62] Habgood M, Grau-Crespo R, Price SL. Substitutional and orientational disorder in organic crystals: a symmetry-adapted ensemble model. Physical Chemistry Chemical Physics. 2011;13(20):9590-600.

[63] Redinha JS, Lopes Jesus AJ. Molecular Recognition and Crystal Growth. In: McEvoy JA, editor. Molecular Recognition: Biotechnology, Chemical Engineering and Materials Applications: Novapublishers; 2011.

[64] Redinha JS, Lopes Jesus AJ. Crystal Growth of Pharmaceuticals from Melt. In: Borisenko E, editor. Crystallization and material science of modern artificial and natural crystals. Rijeka: InTech; 2012.

[65] Pascard C, Tran Huu Dau E, Manoury P, Mompon B. Betaxolol hydrochloride: 1-{4-[2-(cyclopropylmethoxy)ethyl]phenoxy}-3-isopropylamino-2-propanol hydrochloride, C18H30NO3+.Cl. Acta Crystallographica, Section C: Crystal Structure Communications. 1984;40(8):1430-2.

[66] Lopes Jesus AJ, Nunes SCC, Ramos Silva M, Matos Beja A, Redinha JS. Erythritol: Crystal growth from the melt. International Journal of Pharmaceutics. 2010;388(1-2): 129-35.

[67] Lopes Jesus AJ, Redinha JS. On the structure of erythritol and L-threitol in the solid state: An infrared spectroscopic study. Journal of Molecular Structure. 2009;938(1-3): 156-64.

[68] Yu L, Reutzel-Edens SM, Mitchell CA. Crystallization and Polymorphism of Conformationally Flexible Molecules: Problems, Patterns, and Strategies. Organic Process Research & Development. 2000 2012/09/14;4(5):396-402.

[69] Lopes Jesus AJ, Tomé LIN, Rosado MTS, Leitão MLP, Redinha JS. Conformational study of erythritol and threitol in the gas state by density functional theory calculations. Carbohydrate Research. 2005;340(2):283-91.

[70] Lopes Jesus AL, Tomé LIN, Eusébio MES, Redinha JS. Determination of the Enthalpy of Solute-Solvent Interaction from the Enthalpy of Solution: Aqueous Solutions of Erythritol and L-Threitol. Journal of Physical Chemistry B. 2006 May 11, 2006;110(18): 9280-5.

[71] Ceccarelli C, Jeffrey GA, McMullan RK. A Neutron-Diffraction Refinement of the Crystal-Structure of Erythritol at 22.6 K. Acta Crystallographica Section B. 1980;36:3079-83.

[72] Kopf J, Morf M, Zimmer B, Haupt ETK, Jarchow O, Köll P. The crystal and molecular structure of threitol. Carbohydrate Research. 1993;247:119-28.

[73] Jeffrey GA, Kim HS. Conformations of the alditols. Carbohydrate Research. 1970;14(2):207-16.

[74] Kitamura M. Polymorphism in the crystallization of L-glutamic acid. Journal of Crystal Growth. 1989;96(3):541-6.

[75] Kitamura M. Controlling factor of polymorphism in crystallization process. Journal of Crystal Growth. 2002;237-239:2205-14.

[76] Davey RJ, Blagden N, Potts GD, Docherty R. Polymorphism in Molecular Crystals: Stabilization of a Metastable Form by Conformational Mimicry. Journal of the American Chemical Society. 1997;119(7):1767-72.

[77] Ono T, ter Horst JH, Jansens PJ. Quantitative Measurement of the Polymorphic Transformation of l-Glutamic Acid Using In-Situ Raman Spectroscopy. Crystal Growth & Design. 2004;4(3):465-9.

[78] Lehmann M, Koetzle T, Hamilton W. Precision neutron diffraction structure determination of protein and nucleic acid components. VII. The crystal and molecular structure of the amino acid L-lysine monohydrochloride dihydrate. Journal of Chemical Crystallography. 1972;2(5):225-33.

[79] Lehmann MS, Nunes AC. A short hydrogen bond between near identical carboxyl groups in the [alpha]-modification of l-glutamic acid. Acta Crystallographica, Section B: Structural Science. 1980;36(7):1621-5.

[80] Kim CK, Park B-H, Lee HW, Kim CK. Comprehensive Studies on the Free Energies of Solvation and Conformers of Glycine: A Theoretical Study. Bulletin of the Korean Chemical Society. 2011;32(6):1985 - 92.

[81] Peng CY, Ayala PY, Schlegel HB, Frisch MJ. Using redundant internal coordinates to optimize equilibrium geometries and transition states. Journal of Computational Chemistry. 1996;17(1):49-56.

[82] Hess B, Kutzner C, van der Spoel D, Lindahl E. GROMACS 4: Algorithms for Highly Efficient, Load-Balanced, and Scalable Molecular Simulation. Journal of Chemical Theory and Computation. 2008;4(3):435-47.

[83] Schuttelkopf AW, van Aalten DMF. PRODRG: a tool for high-throughput crystallography of protein-ligand complexes. Acta Crystallographica Section D. 2004;60(8): 1355-63.

[84] Cohen S, Marcus Y, Migron Y, Dikstein S, Shafran A. Water sorption, binding and solubility of polyols. Journal of the Chemical Society, Faraday Transactions. 1993;89(17):3271-5.

[85] Gilli G, Gilli P. Towards an unified hydrogen-bond theory. Journal of Molecular Structure. 2000;552(1-3):1-15.